Applied Electromagnetics in Materials 1 (1990) 59–64
Elsevier

APPLICATION OF THE VORONOI-DELAUNAY TRANSFORMATION METHOD TO EIGEN VALUE PROBLEMS

Yoshifuru SAITO, Yoshihiro NAKAZAWA, and Seiji HAYANO

College of Engineering, Hosei University, 3-7-2 Kajino, Koganei, Tokyo 184, Japan

Received 19 October 1989

In the present paper, we exploit the Voronoi–Delaunay transformation method whereby the solution of the Delaunay system can be obtained by transforming the solution of the Voronoi system. This Voronoi–Delaunay transformation method is now applied to eigen value problems in electromagnetic fields. As a result, it is revealed that the computation of eigen values can be carried out in an extremely efficient manner.

1. Introduction

A geometric duality between the Delaunay triangles and Voronoi polygons has been utilized to implement a dual energy approach [1–3]. This method requires the use of a single potential to establish the upper and lower bounds of solutions, whereas the conventional dual energy finite element approach requires the use of two different types of potentials i.e., vector and scalar [4–6]. Therefore, the conventional dual energy approach provides only an improved functional, but the geometric dual energy method is capable of providing the improved functional as well as improved local solutions. Even if a single type of potential is required to implement the dual energy approach, this geometric dual energy method has been compelled to solve the two independent systems i.e., Voronoi and Delaunay.

In order to overcome this deficiency, in this paper, we exploit the Voronoi–Delaunay transformation method whereby the solution vector of the Delaunay system can be obtained by transforming the solution of the Voronoi system. Thereby, only the Voronoi system of equations has to be solved to implement the dual energy approach. This Voronoi–Delaunay transformation method is now applied to eigen value problems in electromagnetic fields. As a result, it is shown that the eigen values can be obtained by this Voronoi–Delaunay transformation method in an extremely efficient manner. Simple examples suggest that our Voronoi–Delaunay transformation method is more accurate than the conventional first order triangular finite element method by an order of magnitude.

2. Voronoi–Delaunay transformation method

2.1. Basic field equation

Typical examples of eigen value problems in electromagnetic fields appear in the computation of higher order waveguide modes as well as the evaluation of eddy current distributions. The eigen values in waveguide problems correspond to the operating resonance frequencies, and those in eddy current problems correspond to the time constants of the system. In this paper, the eigen value problem in scalar wave equation is selected as an example.

The axial field components in propagating modes of a uniform and perfectly conducting waveguide satisfy the Helmholtz equation

$$\frac{\partial^2 \phi}{\partial x^2} + \frac{\partial^2 \phi}{\partial y^2} + k_c^2 \phi = 0 , \tag{1}$$

where k_c is the cutoff wavenumber. This cutoff

wavenumber k_c is related to k_0 $[=\omega\sqrt{\mu_0\varepsilon_0}]$ (free space wavenumber) and the propagation constant γ in the direction of z-axis by

$$k_c^2 = k_0^2 - \gamma^2 . \tag{2}$$

ϕ in (1) stands for the axial field components E_z or H_z for TM or TE modes, respectively. For TM modes, (1) is subject to Dirichlet boundary conditions, and for TE modes, it is subject to Neumann boundary condition at the perfect conductor, respectively. To evaluate the waveguide modes, the eigen vectors of (1) are being calculated numerically by means of the finite difference or finite element methods [7–9].

2.2. Locally orthogonal form

A method of locally orthogonal discretization is presented in refs. [1] and [2]. The key concept in this procedure is to exploit the geometric duality that exists between Delaunay triangles and Voronoi polygons. Delaunay triangles and Voronoi polygons are related by the fact that vertices of the Voronoi polygons are the circumcenters of the Delaunay triangles. As explained in ref. [1] and illustrated in fig. 1, one of the features of this Voronoi–Delaunay duality is that the sides of the Voronoi polygons are perpendicular to the sides of the Delaunay triangles. This relationship leads to a locally orthogonal coordinate system as shown in fig. 1. When the vertices i, j of the Delaunay triangle and the vertices k, l of the Voronoi polygon are chosen as node points, the following interpolating function may be assumed

$$\phi = a_0 + a_1 x + a_2 y + a_3 xy . \tag{3}$$

Application of (3) to the nodes i, j, k, l in fig. 1 yields

$$\begin{vmatrix} \phi_i \\ \phi_j \\ \phi_k \\ \phi_l \end{vmatrix} = \begin{vmatrix} 1 & 0 & a/2 & 0 \\ 1 & 0 & -a/2 & 0 \\ 1 & -b & 0 & 0 \\ 1 & c & 0 & 0 \end{vmatrix} \begin{vmatrix} a_0 \\ a_1 \\ a_2 \\ a_3 \end{vmatrix} \tag{4}$$

Equation (4) suggests that the coefficients a_0, a_1, a_2, a_3 in (3) cannot be uniquely determined. This means that two complete but independent sets of nodal variables must be defined: one is located at the vertices of Delaunay triangles; and the other is located at the vertices of Voronoi polygons. A simple Lagrange interpolation between nodes i and j in fig. 1 yields a trial function for the Delaunay system as

$$\phi = \frac{1}{2}(\phi_i + \phi_j) + (\phi_i - \phi_j)\frac{y}{a} , \tag{5}$$

where a is the distance between the nodes i and j [1–4]. On the other side, a trial function for the Voronoi system is given by

$$\phi = [(c\phi_k + b\phi_l) + (\phi_l - \phi_k)x]/(b + c) , \tag{6}$$

where the distances b and c are shown in fig. 1 [1/4].

According to these two independent interpolating functions (5) and (6), the governing equation (1) may be reduced to a one-dimensional equation in either the Delaunay or in the Voronoi sets of variables:

$$\frac{\partial^2\phi}{\partial x^2} + \frac{1}{2}k_c^2\phi = 0 , \tag{7}$$

$$\frac{\partial^2\phi}{\partial y^2} + \frac{1}{2}k_c^2\phi = 0 , \tag{8}$$

on a locally orthogonal x–y coordinate system shown in fig. 1.

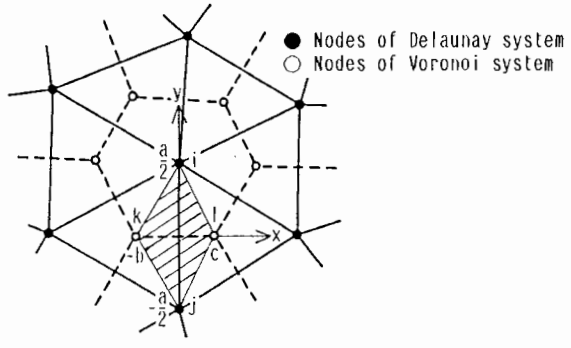

Fig. 1. Voronoi–Delaunay diagram and locally orthogonal coordinate system.

2.3. Functionals and nodal equations

In the Delaunay system, the derivative $\partial\phi/\partial y$ is common to the adjacent Delaunay triangles so that a functional $F(\phi)$ for the Delaunay system is

given by

$$F(\phi) = \int\int \left\{ (\partial\phi/\partial y)^2 - \frac{1}{2} k_c^2 \phi^2 \right\} \mathrm{d}x\, \mathrm{d}y \,. \tag{9}$$

After substituting (5) into (9) and integrating over the region enclosed by *i-k-j-l* in fig. 1, we can obtain the functional $F(\phi)$ for the Delaunay system. By taking an extremum of this functional $F(\phi)$, a nodal equation for the node i in fig. 1 can be obtained as

$$\left[\frac{b}{a} + \frac{c}{a} \right] (\phi_i - \phi_j) - \left(\frac{k_c^2}{48} \right) a(b+c)[7\phi_i + 5\phi_j] = 0 \,. \tag{10}$$

Thus, an entire Delaunay system of equations is represented by

$$[A_D - k_c^2 B_D] \Phi_D = 0 \,, \tag{11}$$

where A_D, B_D are the coefficient matrices corresponding to the first and second terms on the left of (10); and Φ_D is the eigen vector of Delaunay system, respectively.

In the Voronoi system, the derivative $\partial\phi/\partial x$ is common to the adjacent Delaunay triangles, this leads to a functional $G(\phi)$ for the Voronoi system:

$$G(\phi) = -\int\int \{ (\partial\phi/\partial x)^2 - \frac{1}{2} k_c^2 \hat{\phi}^2 \} \mathrm{d}x\, \mathrm{d}y \,, \tag{12}$$

where $\hat{}$ refers to the prescribed values.

After substituting (6) into (12) and integrating over the region enclosed by *i-k-j-l* in fig. 1, we can obtain the functional $G(\phi)$ for the Voronoi system. By taking an extremum of this functional $G(\phi)$, a nodal equation for the node k in fig. 1 can be obtained as

$$(\phi_k - \phi_l) / \left\{ \frac{b}{a} + \frac{c}{a} \right\} - \left(\frac{k_c^2}{2} \right) a(b+c)\phi_k = 0 \,. \tag{13}$$

Thus, an entire Voronoi system of equations is represented by

$$[A_v - k_c^2 B_v] \Phi_v = 0 \,, \tag{14}$$

where A_v, B_v are the coefficient matrices corresponding to the first and second terms on the left of (13); Φ_v is the eigen vector of Voronoi system, respectively.

2.4. Voronoi–Delaunay transformation

The Voronoi system of equations has been derived satisfying the continuity of normal derivative $\partial\phi/\partial n$ between the adjacent Delaunay triangles. However, as shown in fig. 2(a), it is obvious that the tangential derivative components $\partial\phi/\partial t$ are included in the entire vector Φ_v of Voronoi system. The nodal variables which represent the tangential derivative components are essentially located at the vertices of Delaunay triangles. The original governing equation (1) has been already discretized by the Voronoi discretization method so that the discretized problem region is governed only by a Laplace equation and not the original governing equation (1), viz.,

$$\nabla^2 \phi = 0 \,, \tag{15}$$

must be satisfied by the nodal variables of Delaunay system. Hence, by means of the Delaunay discretization (10), the nodal variable ϕ_i in fig. 2(b) can be represented in terms of the nodal variables of Voronoi system as

$$\begin{aligned} &\frac{1}{2} [(\cot\alpha_5 + \cot\beta_2)\phi_k + (\cot\alpha_1 + \cot\beta_3)\phi_l \\ &\quad + (\cot\alpha_2 + \cot\beta_4)\phi_n + (\cot\alpha_3 + \cot\beta_5)\phi_q \\ &\quad + (\cot\alpha_4 + \cot\beta_1)\phi_r] \\ &= \frac{1}{2} \left[\sum_{j=1}^{5} (\cot\alpha_j + \cot\beta_j) \right] \phi_i \,, \end{aligned} \tag{16}$$

where the nodal variables ϕ_k, ϕ_l, ϕ_n, ϕ_q, ϕ_r and angles α_1–α_5, β_1–β_5 are shown in fig. 2(b).

Thus, by means of (16), the vector Φ_D of Delaunay system can be represented in terms of the connection matrix C and the vector Φ_V of Voronoi system as

$$\Phi_D = C\Phi_V \,. \tag{17}$$

By means of (17), the Delaunay system of equations (11) is transformed into the Voronoi system:

$$[C^T A_D C - k_c^2 C^T B_D C] \Phi_V = 0 \,. \tag{18}$$

Thereby, the rearranged resultant system of

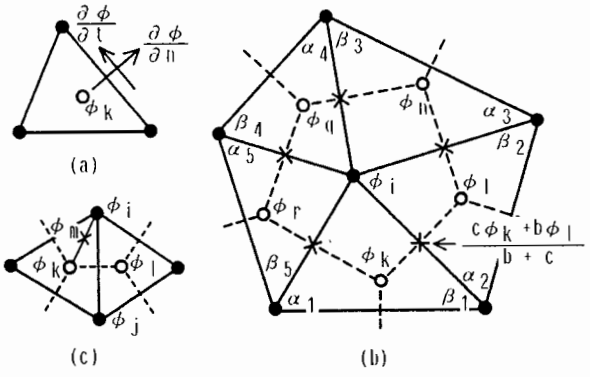

Fig. 2. (a) The normal derivative $\partial\phi/\partial n$ and tangential derivative $\partial\phi/\partial t$.
(b) Transformation from the Voronoi nodal variables to Delaunay nodal variables.
(c) Location to the mid point nodal variable ϕ_m.

equations becomes

$$[D - k_c^2]\Phi_V = 0\,, \tag{19}$$

where

$$D = \frac{1}{2}\,[B_V^{-1}A_V + (C^T B_D C)^{-1}(C^T A_D C)]\,. \tag{20}$$

Each of the eigen values computed by the Delaunay (11) and Voronoi (14) systems takes different values depending on their own systems, but the eigen value computed by (19) may take their averaged value. This means that the promising eigen value may be computed from (19) even if a small number of nodes is employed. Further improvement of the eigen vector Φ_V in (19) is possible when we consider the nodal variables located at the mid points between the vertices of Voronoi polygons and Delaunay triangles. The mid point vector Φ_M can be represented in terms of the vectors Φ_V and Φ_D as

$$\Phi_M = C_{DM}\Phi_D + C_{VM}\Phi_V\,, \tag{21}$$

where C_{DM}, C_{VM} are the interpolating matrices between the vertices of Voronoi polygon and Delaunay triangle. For example, a mid point nodal variable ϕ_m in fig. 2(c) is given by

$$\phi_m = \frac{1}{2}\,\phi_i + \frac{1}{2}\,\phi_k\,. \tag{22}$$

By, means of (17), (21) is reduced into

$$\Phi_M = (C_{DM}C + C_{VM})\Phi_V\,. \tag{23}$$

The vector Φ_M in (23) has improved accuracy because the vector Φ_M takes into account both the rate of changes for the normal ($\partial\phi/\partial n$) and tangential ($\partial\phi/\partial t$) directions in fig. 2(a).

2.5. Examples

Figure 3 shows a rectangular waveguide which has been selected as an initial test example. Because of symmetry, we computed only the hatched region of this waveguide.

Figure 4(a) shows the convergence properties

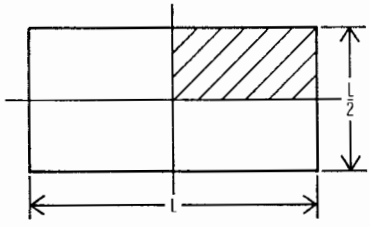

Fig. 3. A rectangular waveguide. Because of its symmetry, only the hatched region is computed.

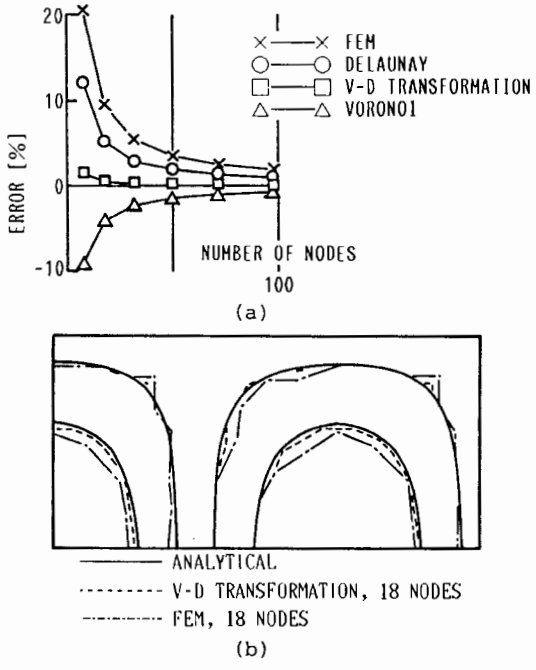

Fig. 4. (a) Convergence properties of eigen value by the Delaunay, Voronoi, Voronoi–Delaunay transformation (V–D transformation) and FEM in TM_{31} mode.
(b) Field distribution in TM_{31} mode.

of eigen values by the Delaunay (11), Voronoi (14) and Voronoi–Delaunay transformation (19) methods for TM_{31} mode. For comparison, the results of conventional first order triangular finite element using the same mesh as Delaunay system method are also shown in fig. 4(a). By considering fig. 4(a), it is obvious that the Voronoi–Delaunay transformation method yields a far better result even if a small number of nodes is employed. Figure 4(b) shows the field distribution of this mode computed by the Voronoi–Delaunay transformation and conventional first order finite element methods. The result in fig. 4(b) reveals that Voronoi–Delaunay transformation method (23) provides an excellent field distribution.

Figure 5(a) shows the convergence properties of eigen value by the Delaunay (11), Voronoi (14) and Voronoi–Delaunay transformation (19) methods for TE_{22} mode. Figure 5(b) shows the field distributions of TE_{22} mode computed by the Voronoi–Delaunay transformation method (23) and the conventional first order finite element method using the same mesh as Delaunay system, respectively. Our Voronoi–Delaunay transformation method (23) provides a far better field distribution compared with those of the finite element method, even if a small number of node points is employed. The results of figs. 5(a) and 5(b) demonstrate that the Voronoi–Delaunay transformation method is quite effective for the TE mode problems.

Finally, we show the usefulness of our Voronoi–Delaunay transformation method for finding the higher order operating mode. Figure 6(a)

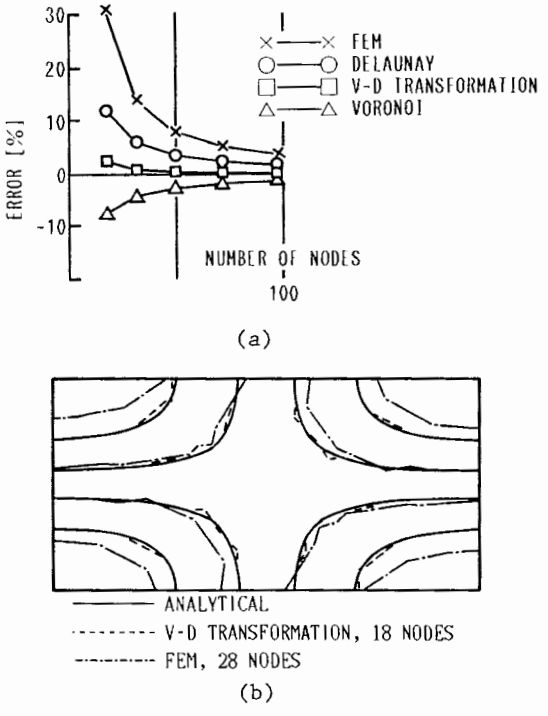

Fig. 5. (a) Convergene properties of eigen value by the Delaunay, Voronoi, Voronoi–Delaunay transformation (V–D transformation) and FEM in TE_{22} mode.
(b) Field distribution in TE_{22} mode.

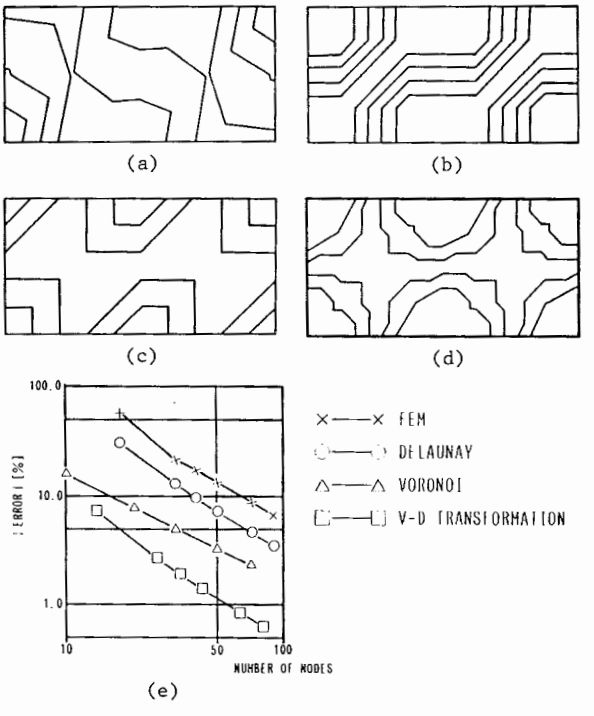

Fig. 6. (a) TE_{42} mode computed by FEM using 15 nodal variables.
(b) TE_{42} mode computed by the Voronoi system eigen vector Φ_V in (19), where 8 nodal variables are employed.
(c) TE_{42} mode computed by the Delaunay system eigen vector Φ_D in (17).
(d) TE_{42} mode computed by the Voronoi–Delaunay transformation method (23).
(e) Convergence properties of TE_{42} mode eigen value.

shows a TE mode field distribution computed by the conventional first order finite element method using a Delaunay triangular mesh. Obviously, it is difficult to find the operating mode of this waveguide from the result in fig. 6(a). Figures 6(b) and 6(c) show the field distribution obtained from the Voronoi system eigen vector in (19) and its associated Delaunay eigen vector in (17), respectively. From the results in figs. 6(b) and 6(c), it is difficult to decide on the operating mode. However, by means of the hybrid scheme of (21) or (23), a combination of both field distributions in figs. 6(b) and 6(c) yields a fairly clear result as shown in fig. 6(d). Figure 6(d) reveals that this waveguide is now operating in TE_{42} mode. In fig. 6(a), it was required to employ 15 nodal points for the first order triangular mesh, but only 8 nodal points for the Voronoi polygonal mesh were employed to reach the result in fig. 6(d). Nevertheless, the result in fig. 6(d) yields a clear field distribution compared with those of fig. 6(a). This fact can be confirmed by considering the convergence properties of eigen values shown in fig. 6(e).

Thus, our Voronoi–Delaunay transformation method is far superior than the conventional first order finite element method for eigen value problems.

3. Conclusions

As shown above, we have exploited a new method that requries only one system of equations to implement a dual energy approach, while the conventional locally orthogonal discretization method requires the solutions of two-independent systems of equations i.e., Voronoi and Delaunay. This new method has been applied to the computation of the eigen value problem in electromagnetic fields. As a result, the example problems have shown that our new method provides the far better results compared with those of the conventional first order finite element method.

References

[1] Y. Saito et al., Faster magnetic field computation using locally orthogonal discretization, IEEE Trans. Magn. Vol. MAG-22, No. 5 (1986) 1057.

[2] Y. Saito et al., Modeling of magnetization characteristics and faster magnetodynamic field computation, J. Appl. Phys. 63(8) (1988) 3174.

[3] Y. Saito et al., An efficient computation of saturable magnetic field problem using locally orthogonal discretization, IEEE Trans. Magn., Vol. MAG-24, No. 6 (1988) 3138.

[4] J. Penman et al., Complementary and dual energy finite element principles in magnetostatics, IEEE Trans. Magn. Vol. MAG-18, No. 2 (1982) 319.

[5] P. Hammond et al., Dual finite-element calculations for static electric and magnetic fields, Proc. IEE, Pt.A, Vol. 130, No. 3 (1983) 105.

[6] P. Hammond et al., Calculation of inductance and capacitance by means of dual energy principles, Proc. IEE, Vol. 123, No. 6 (1976) 554.

[7] M.J. Bearbien et al., An accurate finite-difference method for higher order waveguide modes. IEEE Trans. Microwave Theory and Techniques, Vol. MIT-16, No. 12 (1968) 1007.

[8] P. Silvester, A general high-order finite-element waveguide analysis program, IEEE Trans. Microwave Theory and Techniques, Vol. MIT-17, No. 4 (1969) 204.

[9] M. Israel et al., An efficient finite element method for nonconvex waveguide based on Hermitian polygons, IEEE Trans. Microwave Theory and Techniques, Vol. MIT-35, No. 11 (1987) 1019.